Structural determinants of phorbol ester binding activity of the C1a and C1b domains of protein kinase C theta

Agnes Czikora[a], **Satyabrata Pany**[b], **Youngki You**[b], **Amandeep S. Saini**[a], **Nancy E. Lewin**[a], **Gary A. Mitchell**[a], **Adelle Abramovitz**[a], **Noemi Kedei**[a], **Peter M. Blumberg**[a,*], **Joydip Das**[b,*]

[a]Laboratory of Cancer Biology and Genetics, Center for Cancer Research, National Cancer Institute, Bethesda, MD 20892, United States

[b]Department of Pharmacological and Pharmaceutical Sciences, College of Pharmacy, University of Houston, Houston, TX 77204, United States

Abstract

The PKC isozymes represent the most prominent family of signaling proteins mediating response to the ubiquitous second messenger diacylglycerol. Among them, PKCθ is critically involved in T-cell activation. Whereas all the other conventional and novel PKC isoforms have twin C1 domains with potent binding activity for phorbol esters, in PKCθ only the C1b domain possesses potent binding activity, with little or no activity reported for the C1a domain. In order to better understand the structural basis accounting for the very weak ligand binding of the PKCθ C1a domain, we assessed the effect on ligand binding of twelve amino acid residues which differed between the C1a and C1b domains of PKCθ. Mutation of Pro^9 of the C1a domain of PKCθ to the corresponding Lys^9 found in C1b restored in vitro binding activity for [^{3}H]phorbol 12,13-dibutyrate to 3.6 nM, whereas none of the other residues had substantial effect. Interestingly, the converse mutation in the C1b domain of Lys^9 to Pro^9 only diminished binding affinity to 11.7nM, compared to 254 nM in the unmutated C1a. In confocal experiments, deletion of the C1b domain from full length PKCθ diminished, whereas deletion of the C1a domain enhanced 5-fold (at 100 nM PMA) the translocation to the plasma membrane. We conclude that the Pro^{168} residue in the C1a domain of full length PKCθ plays a critical role in the ligand and membrane binding, while exchanging the residue (Lys^{240}) at the same position in C1b domain of full length PKCθ only modestly reduced the membrane interaction.

Keywords

Diacylglycerol; PMA; PKCθ; Binding affinity; C1 a domain; Phorbol ester; Membrane translocation

1. Introduction

Protein kinase C (PKC) is a family of serine/threonine specific protein kinases that are a major target of the tumor-promoting phorbol esters and that play a crucial role in cellular signal transduction via the second messenger diacylglycerol (DAG) [1, 2]. The PKC superfamily contains nine genes which are further divided into the conventional isoforms (α, βI, βII and γ), which are regulated by calcium as well as by DAG, the novel isoforms (δ, ε, θ and η), which are regulated by DAG but not by calcium, and the atypical (ζ/ι) PKCs, which are regulated by neither. DAG is a lipid second messenger that selectively interacts with proteins at C1 domains, shifting the C1 domain from intramolecular interactions to those with the membrane. DAG thus drives conformational change in its target proteins as well as their membrane translocation. This latter effect, by bringing the protein into proximity with signaling complexes, substrates and regulators, represents an important mechanism for target activation [3]. A further level of complexity is that prolonged activation of cPKC and nPKC isozymes with phorbol ester leads to their dephosphorylation and degradation [4,5]. These and other factors drive a rich pharmacology for C1 domain targeted ligands, with ingenol 3-angelate approved by the FDA for actinic keratosis and bryostatin 1 in clinical trials for cancer and Alzheimer's disease.

The structure of all PKC isozymes consists of an N-terminal regulatory and a C-terminal catalytic domain. Within the regulatory domain of the classical and novel PKCs are tandem C1 domains, designated C1a and C1b. These C1 domains are zinc-finger structures of approximately 50 amino acids with a conserved pattern of cysteine and histidine residues (H-$\times_{12}$-C-$\times_2$-C-$\times_{13/14}$-C-$\times_2$-C-$\times_4$-H-$\times_2$-C-$\times_7$-C) (Fig. 1) [6,7]. Different C1 domains may differ both in ligand selectivity and in functional impact on PKC behavior. The C1b domain of PKCβ has appreciably lower affinity for DAG than does the C1 domain of the PKCδ [8], attributable to the presence of Tyr rather than Trp at position 22 in their C1b domain [9]. Little difference is seen in the response to phorbol ester, in contrast. For PKCδ constructs in which either the C1a or C1b domains were deleted, the C1a deleted constructs show no difference from wild-type in in vitro affinity for either phorbol ester or DAG, whereas the C1b deleted constructs showed a 47-fold loss of phorbol ester binding affinity and a 180-fold loss of affinity for DAG [10]. In intact cells, both these deletion constructs [10] and mutants of PKCδ in which one or the other C1 domain was inactivated showed that the C1b domain played the predominant role in the translocation of PKCδ in response to phorbol ester [11]. In contrast, whereas membrane translocation for some ligands, e.g. octylindolactam V, was like PMA in showing predominant dependence on the C1b domain for PKCδ translocation, for other ligands such as bryostatin 1 or mezerein inactivating mutations in either C1 domain were equivalent [12].

The crystal structure of the PKCδ C1b domain as well as physical chemical studies and modeling of C1 domains have provided insights into the nature of ligand-receptor interaction and the regions within the domain that govern the insertion of PKC into the membranes [13, 14, 15]. The C1 domain is constituted of two β sheets and a α helix. The β sheets form a pocket in which phorbol esters and DAG bind. The binding pocket is comprised of a cluster

of hydrophobic residues on the top of the domain, while the middle region is composed mainly of positively charged residues [13].

The literature has suggested that PKCθ is unusual in that its C1a domain either is very weak in phorbol ester binding activity (900 nM versus 3.4 nM for the C1b domain) [16] or is very much less active than its C1b domain for its interactions with diacylglycerol (1900 versus 26 nM, assayed by surface plasmon resonance) [17]. A less clear picture emerges when the roles of the C1 domains are assessed in the context of the full protein. There, while mutations reducing affinity in the C1a domain of PKCθ had little effect, those in the C1b domain of PKCθ caused only a 6–14-fold reduction in affinity (as measured by surface plasmon resonance) [17].

In addition to the unusual nature of its C1 domains, PKCθ is of particular biological interest for its recruitment to the immunological synapse [18], where it plays a critical role in T-cell activation that mediates non-redundant functions in T-cell receptor (TCR) signaling, including T-cell activation, proliferation, differentiation and survival [18,19]. An overactive immune system is responsible for different immunity-related complications such as arthritis [20], asthma [21], multiple sclerosis [22, 23] and Type-1 diabetes [24]. PKCθ knockout mice were found to be protected from asthma and arthritis, indicating the importance of PKCθ in immune responses [20, 22, 25, 26]. Several studies described a role of PKCθ in cancer settings as well. In gastrointestinal stroma tumors and Ewing's sarcoma PKCθ could be used as a specific marker of the disease [27, 28, 29]. These studies suggest that PKCθ overexpression facilitates the diagnostics of tumors even in the case where traditional markers are absent. However, its role in the pathogenesis is still unclear.

In previous studies, we have examined in detail the structure of the PKCθ C1b domain, for comparison with that of PKCδ. PKCθ C1b has a high sequence homology (80%) with PKCδ C1b. The crystal structures of PKCδ C1b and PKCθ C1b likewise revealed remarkable similarity of the overall structure [30]. However, superimposition of the PKCθ C1b structure with the PKCδ C1b showed that the activator-binding pocket opening of PKCθC1b was slightly narrower than was that of the PKCδC1b.

In the present paper, we have examined the structural features contributing to the weak phorbol ester binding activity of the C1a domain of PKCθ and its contributions to translocation of PKCθ in response to phorbol ester. We confirmed that the C1a motif of PKCθ binds phorbol ester weakly and that Pro^9 in the PKCθ C1a motif is the primary contributor to this weak binding. We further excluded many of the other differences in residues between the C1a and C1b domains as contributing to the weak binding potency of the C1a domain. On the other hand, change of the corresponding Lys^9 residue in the PKCθ C1b domain to the Pro^9 residue present in the C1a domain had appreciably less effect, suggesting that other residues in the C1b domain help to preserve binding affinity in the presence of Pro^9. Analysis of the behavior of the individual C1 domains of PKCθ was complemented by exploration of their role in translocation of the full length PKCθ in response to phorbol esters. Using confocal microscopy, we found that the C1b domain from full length PKCθ was essential for translocation. The C1a domain showed no evidence of contributing to translocation, whereas its deletion or replacement with a second C1b domain

enhanced translocation. Consistent with these results, mutation of the Pro^{168} residue to Lys in the C1a domain of full length PKCθ (P9K as numbered in the C1a domain) enhanced translocation whereas exchanging the residue (Lys^{240}) at the corresponding position in the C1b domain of full length PKCθ reduced translocation.

2. Materials and methods

2.1. Materials

[^{3}H]Phorbol 12, 13-dibutyrate ([^{3}H]PDBu) (13.5 Ci/mmol) was obtained from Perkin Elmer Life Sciences. PDBu and phorbol 12-myristate 13-acetate (PMA) were purchased from LC Laboratories (Woburn, MA). Phosphatidyl-L-serine (PS) and phosphatidylcholine (PC) were from Avanti Polar Lipids (Alabaster, AL). Dimethyl sulfoxide (DMSO) was purchased from Sigma – Aldrich (St. Louis, MO). LNCaP human prostate cancer cells, fetal bovine serum (FBS), RPMI 1640 medium, and L-glutamine were from American Type Culture Collection (Manassas, VA). Reagents used for culturing bacteria (LB Broth, LB agar plates with different selection of antibiotics, etc.) were from K-D Medical, Inc. (Columbia, MD). The oligonucleotide primers used for polymerase chain reaction (PCR) were obtained from Integrated DNA Technologies (Coralville, IA), and site-directed mutagenesis was from Invitrogen.

2.2. Construction of deletion and substitution mutants

The wild type full-length PKCθ (θ/WT) in pEGFP-N1 vector was used to construct two domain deletion, two domain substitution and two amino acid substitution mutants either by PCR based recombination or by site-directed mutagenesis. The domain structure of the PKCθ wild-type and the sites of mutations are shown in Fig. 2. Mutants are designated θ/ C1a (in which θC1a was deleted), θ/ C1b (in which θC1b was deleted), θ/C1a-C1a (in which θC1b was substituted with θC1a), θ/C1b-C1b (in which θC1a was substituted with θC1b), θ/P168K (in which Pro 168 of θC1a was substituted with Lys) and θ/K240P (in which Lys 240 amino acid of θC1b domain was substituted with Pro).

Additionally, twenty amino acid substitution mutants (13 single, 6 double and 1 triple) of the isolated θC1a (amino acids 160–209 in θ/WT) and θC1b (amino acids 232–281 in θ/WT) domains in the pGEX-2TK vector were constructed by site-directed mutagenesis. Mutants of ΘC1a domain are designated as θC1a/F167Y (F8Y), θC1a/P168K (P9K), θC1a/Q169S (Q10S), θC1a/S174E (S15E), θC1a/V175H (V16H), θC1a/H177G (H18G), θC1a/E178T (E19T), θC1a/F179L (F20L), θC1a/V180L (V21L), θC1a/A195M (A36M), θC1a/P168K-V175H (P9K-V16H), θC1a/P168K-E178T (P9K-E19T), θC1a/H177G-E178T (H18G-E19T), θC1a/N184A-K185R (N25A-K26R) and θC1a/H177G-E178T-V180L (H18G-E19T-V21L). Mutants of θC1b domain are referred as θC1b/K240P (K9P), θC1b/L252V (L21V), ΘC1b/M267A (M36A), θC1b/K240P-T250E (K9P-T19E), and θC1b/K240P-M267A (K9P-M36A). Point mutations of the amino acid residues were introduced using the GeneArt^R site-directed mutagenesis system (Invitrogen) according to the manufacturer's instructions. DNA sequencing of the mutant constructs were carried out to confirm the correct sequences (SeqWright, Houston, TX and Center for Cancer Research Genomics Core, NCI, National Institute of Health).

2.3. Protein expression and purification for mutants

Bacterial expression was carried out as reported earlier [30]. Briefly, cells were lysed in lysis buffer ($1\times$ PBS, 1 mg/ml lysozyme, and 10 mM DTT and protease inhibitor) at 4 °C for 1 h and then sonicated for 2 min at 30% amplitude with a 5 s on/off cycle. The supernatant was collected following a 15 min centrifugation (15,000 g) at 4 °C. 1 ml of glutathione Sepharose™ 4B resin, equilibrated with $1\times$ PBS, was added to the supernatant and incubated at room temperature for 2h. The mixture was transferred to a 10 ml polypropylene column and the flowthrough was collected. The resin was washed with 50 column volumes of wash buffer ($1\times$ PBS) and incubated for 16 h with 50 unit of thrombin in 300 μl of $1\times$ PBS at room temperature. Protein was eluted with 10 column volumes of elution buffer ($1\times$ PBS). The eluted fractions were pooled and concentrated using an Amicon filter at 4 °C and injected onto the Superdex™ 75 (GE Healthcare Bio-Sciences, Marlborough, MA) column pre-equilibrated in buffer containing 50 mM Tris-Cl, pH 7.2, 150 mM NaCl. The protein of interest was eluted based on its molecular weight with the same equilibrium buffer. The eluted protein was further concentrated, its concentration was measured, and it was then stored at −80 °C. SDS-PAGE analysis of the purified mutated proteins showed that each displayed a single band corresponding to ~7 kDa.

2.4. In vitro [^{3}H]PDBu assays

The dissociation constants (K_d values) of [^{3}H]PDBu binding to the individual C1 domains of the PKCθ protein were measured using the polyethylene glycol precipitation assay developed in our laboratory as described in detail previously [31]. Triton X-100, included in assays, did not exceed 0.003%. All values represent the mean ± SEM of at least triplicate independent experiments, where all points in each dose response curve in each experiment were measured in triplicate.

2.5. Confocal analysis of GFP-labeled PKCθ proteins

LNCaP cells were plated at a density of 100,000 cells/plate on Ibidi μ-dishes (Ibidi, LLC, Verona, WI) and subcultured at 37 °C in RPMI 1640 medium supplemented with 10% FBS and 2 mm L-glutamine. After 48 h in culture, cells were transfected with GFP-tagged recombinant constructs, using X-tremeGENE HP DNA transfection reagent (Sigma) according to the manufacturer's recommendations. After 24 h, the cells were treated as indicated with 100 nM, 1 μM and 10 μM of PMA in confocal medium (Dulbecco's Modified Eagle Medium without phenol red supplemented with 1% FBS), and time-lapse images were collected every 30 s using the Zeiss AIM software. Imaging was with a Zeiss LSM 510 confocal microscopy system (Carl Zeiss, Inc.) with an Axiovert 100 M inverted microscope operating with a 25 mW argon laser tuned to 488 nm. A 63×1.4 NA Zeiss Plan-Apochromat oil-immersion objective was used together with varying zooms (1.4 to 2×). Imaging was performed in the Imaging Core Facility, Center for Cancer Research, Bethesda, MD.

2.6. Quantification of confocal images

In each cell two regions of 4 μm^2 were selected: one each in the cytoplasm and in the cell membrane. Mean intensities of the GFP-tagged constructs in the selected regions were

calculated using the Zeiss AIM software for the images at the different time points; the ratio of the intensities for membrane/cytoplasm was then calculated and normalized to the time 0 values. The increase in the membrane/cytoplasm ratio indicates translocation.

2.7. Statistical analysis

The significance of the data obtained (for PKCθ wild-type and its mutants) from the activator-induced membrane translocation study was assessed using an unpaired two-tail *t*-test. P < 0.05 was considered significant.

2.8. Docking simulation

Phorbol-13-O-acetate was docked into PKCθ C1a (PDB: 2ENN) and C1b (PDB: 4FKD) domains using Sybyl × 2.1. Phorbol-13-O-acetate was drawn using ChemBioDraw 12.0. Pro[9] of the C1a domain and Lys[9] of C1b were mutated to Lys and Pro, respectively using Discovery Studio 4.5 For the docking simulation, the energies of the four C1 domains, C1a WT, C1a P9K, C1b WT, and C1b K9P, were minimized and protomols were created for a docking space for the ligand using Sybyl. Protomols were generated by selecting the specific residues with radius 1.0 Å. The residues were selected based on the phobol-13-O-acetate-bound crystal structure of PKCθ C1b [13, 32]. A Threshold value of 0.35 and a Bloat value of 2.0 were used to create the protomols. After generating the protomol, the docking simulations were performed using the Surflexdock Geom module of Sybyl.

2.9. MD simulation

Molecular dynamics (MD) simulations were conducted on the four simulating systems composed of the C1a WT, C1a P9K, C1b WT, and C1b K9P, each docked with phorbol-13-O-acetate, using the GROMACS 4.6.5 package of programs [33] with Amber99sb force field [34]. For the MD simulation, the conformation that showed the highest docking score was selected. The topology and coordinate files of phorbol-13-O-acetate generated by the Antechamber program in the AMBER tool were converted to GROMACS format using ACPYPE [35]. The models were solvated by TIP3P water molecules [36] with a box distance of 1.3 nm and neutralized by adding Cl^- counter ions. About 8204 to 8496 water molecules were used to solvate the systems. In order to remove steric clashes generated while solvating the system energy minimization was carried out using the steepest descent method until the maximum force (Fmax) was below 100 kJ/mol·nm. After energy minimization, the systems were equilibrated for 1000 ps by position-restrained MD simulation in order to maintain temperature and pressure of systems and relax the solvent. The equilibration was performed in two phases. NVT optimization with 300 K was conducted in the first phase, and the second phase was conducted for NPT optimization with 1 bar. Following the equilibration, the MD production run was conducted using the Berendsen coupling method [37] with 300 K and 1 bar for 5.0 ns for all four systems. The bond lengths were constrained by the LINCS algorithm [38] allowing a time step of 2 fs. The Particle Mesh Ewald (PME) method [39] was used to compute electrostatic interactions. The van der Waals, electrostatic, and coulombic interactions were calculated with a 1 nm cut-off. For data analysis, the atomic coordinates were saved every 10 ps during the MD simulation. The MD trajectories of the four systems were analyzed by GROMACS analysis tools, including g_energy and g_dist. The graphs were plotted by GraphPad Prism 5. The

trajectories and structures were visualized using PyMol v1.7 (Schrodinger, LLC.) and Discovery Studio Visualizer 4.5 (Biovia Inc.).

3. Results

3.1. Phorbol ester binding of PKCθ and its mutants

Most of the C1 domains of conventional and novel PKC isozymes show strong PDBu binding affinities with K_d values in the low nanomolar range [40–42]. The isolated PKCθ C1a domain clearly bound PDBu, but its affinity ($K_d = 250 \pm 40$ nM) was much weaker than that of the isolated PKCθ C1b domain ($K_d = 1.6 \pm 0.5$ nM) (Fig. 3).

Based on comparisons of the sequences of the PKCθ C1a and C1b domains, as well as that of the PKCθ C1b domain, which also shows potent binding, we examined candidate residues in the PKCθ C1a domain that might contribute to its low phorbol ester binding affinity (Fig. 1). The F8Y, P9K, Q10S, S15E, V16H, H18G, E19T, F20L, V21L, A36M, P9K-V16H, P9K-E19T, H18G-E19T, N25A-K26R, and H18G-E19T-V21L mutants in PKCθ C1a as well as the K9P, L21V, M36A, K9P-T19E and K9P-M36A mutants in PKCθ C1b were generated using site directed mutagenesis and their binding affinities for PDBu (K_d) were measured in an in vitro [³H]PDBu binding assay. With a chemically synthesized PKCθ C1a domain, the Pro residue at position 9 in the C1a domain of PKCθ was reported to be an important contributor to its weak binding activity, with replacement by the Lys residue present in the PKCθ C1b domain restoring good affinity [16]. Under our assay conditions, mutation of Pro[9] to Lys[9] in the C1a domain afforded $K_d = 3.6 \pm 0.3$ nM, compared to 1.6 $\pm$ 0.5 for the wild type C1b domain (Table 1). The difference between the C1a and C1b domains is more profound, however. The converse mutation in the C1b domain, replacing Lys[9] with Pro[9], yielded an intermediate binding affinity ($K_d = 11.7 \pm 0.3$ nM), indicating that other residues in the C1a domain confer greater impact on the presence of Pro[9] in the case of the C1a domain than is the case for the C1b domain. Differently expressed, other residues in the C1b domain help mitigate the consequences of the presence of Pro[9]. Nevertheless, the other single residues that we mutated in the PKCθ C1a domain in the presence of the Pro[9] conferred no (V16H, E19T, F20L, H18G, A36M) or very little (V21L, Q10S, S15E) improvement in PDBu binding, as was also the case for the H18G/E19T and N25A/K26R double mutants and the H18G/E19T/V21L triple mutant. Consistent with the good binding by the P9K mutant, the double mutants P9K/V16H and P9K/E19T showed similar or slightly improved binding (Table 1).

3.2. Translocation of the GFP-tagged wild type and mutant PKCθ in living LNCaP cells in response to PMA

To probe the contributions of the C1a and C1b domains to phorbol ester responsiveness in their context in PKCθ, as distinct from their behavior in isolation, we examined the translocation pattern of the full length wild type PKCθ and PKCθ mutants in live cells using confocal microscopy. The mutants of PKCθ either had the C1a or C1b domains deleted, had the C1a domain replaced with a second copy of the C1b domain, had the C1b domain replaced with a second copy of the C1a domain, or had the C1a or C1b domains mutated to express Pro in the 9 position (Fig. 2). We then prepared fusion constructs between GFP and

the wild type and mutant forms of PKCθ. The constructs were transfected into the LNCaP human prostate cancer cell line, a cell line that has been extensively used for the analysis of PKC translocation. The translocation of the overexpressed GFP-PKCθ and its mutants was visualized by confocal microscopy after the addition of 100 nM, 1 μM and 10 μM PMA. Time points at 0 min (before PMA addition) and 5, 10 min after PMA addition are shown (Figs. 4A, 5A, 6A and 7A). Before PMA addition, the constructs displayed a mostly uniform expression throughout the membrane and cytoplasm. The wild type PKCθ translocated in a dose dependent manner after addition of 1 and 10 μM PMA (Fig. 4A, rows 2 and 3; Fig. 4B), with little response after addition of 100 nM PMA (Fig. 4A, row 1; Fig. 4B).

Replacing the C1a domain with a second copy of the C1b domain showed stronger translocation, with response after addition of 100 nM PMA (Fig. 5A), whereas deletion of the C1b domain from full length PKCθ caused complete loss of plasma membrane translocation under our assay conditions (Fig. 5B). The PKCθ chimera in which the C1b domain was replaced with a second copy of the C1a domain showed no translocation after treatment with 1 μM PMA, while after 10 μM PMA we observed a very small but statistically significant increase in the translocation (Fig. 6A). On the other hand, deletion of the C1a domain from the wild type PKCθ construct (the C1a PKCθ chimera) yielded enhanced membrane interaction compared to the wild type (Fig. 6B). A plausible interpretation is the that C1a domain, in the absence of ligand, is involved in intramolecular interactions in PKCθ contributing to a closed conformation [17], and the deletion relieves this constraint. Likewise, increased translocation of the single mutant PKCθ/P168K (mutation in the C1a domain) was observed here compared to wild type, although it did not achieve statistical significance as a result of the large SEM (Fig. 7A, column 1 and Fig. 4A, column 1). This latter enhanced translocation presumably reflects the increased binding of phorbol ester to the C1a P9K mutant. Conversely, the single mutant PKCθ/K240P (C1b domain mutation) showed modestly decreased translocation after 1 μM PMA addition. These data correlate with the modestly decreased PDBu binding affinity of the PKCθ C1b K9P mutant compared to wild type C1b domain.

The live cell imaging confirmed that PKCθ C1b plays the predominant role in the membrane translocation and activation process of PKCθ (Fig. 8). They also highlight the difference with PKCδ, where a construct with the PKCδ C1b domain replaced with a second copy of the PKCδ C1a domain showed weak translocation at 10 μM PMA [10].

3.3. Modeling of the wild-type and the mutant C1a and C1b domain of PKCθ

In order to develop further insight into the structural effects of Pro[9] in the C1a domain on phorbol ester binding, we docked a phorbol ester into the wild type and mutated C1 domains, and then conducted MD simulations over 5.0 ns for the four systems, C1a WT, C1a P9K, C1b WT, and C1b K9P. The phorbol ester was docked into the active site located between the two loops of the C1 domains. The docking poses of the phorbol ester on each C1 domain were slightly different and showed different docking scores. Usually, a higher value of docking score represents higher binding affinity. The C1a P9K showed a higher docking score (3.47) than did the C1a WT (2.37), and the C1b WT (5.27) showed a higher score than did the C1b K9P (4.55). These docking results predict that the mutation of the

Pro[9] in C1a to the Lys[9] increases the affinity of the phorbol ester to the C1a domain and the mutation of the Lys[9] to the Pro[9] reduces the affinity of the phorbol ester in C1b. These predictions are consistent with our experimental binding affinity data.

The potential energies of the four molecular systems were quickly stabilized and remained stable during the 5.0 ns MD simulation (Fig. 9). The potential energy of C1a WT was slightly higher than that of C1a P9K; conversely, the potential energy of C1b WT was less than that of the C1b K9P. At the end of 5.0 ns, the recorded potential energies for C1a WT and C1a P9K were −349,554 kJ/mol and −351,438 kJ/mol respectively. For C1b WT and C1b K9P the values were −342,938 kJ/mol and −341,105 kJ/mol respectively. The potential energy plots, therefore, indicated that the mutation of the Pro[9] or Lys[9] in the C1 domain influences the stability of the protein-ligand complex. While for C1a the mutation of Pro[9] to Lys[9] increased the stability, for C1b the mutation of Lys[9] to Pro[9] reduced the stability.

The snapshots for the four systems at each of three time points are illustrated in Fig. 10 for comparison. In the case of the C1a WT, the phorbol ester moved away from the active site and rotated constantly during MD simulation. In contrast, in C1a P9K, the phorbol ester slightly moved away from the active site, but maintained its pose in the binding cleft during MD simulation. In C1b WT and C1b K9P, the phorbol ester docked into the C1b domain more or less like the phorbol ester in the PKCδ C1b-phorbol ester complex (PDB: 1PTR) [13] and the phorbol ester retained its conformation in the active site of both C1b WT and C1b K9P during the 5.0 ns MD simulation.

To understand the influence of the Pro[9] of the C1a and Lys[9] of the C1b on stabilizing the phorbol ester in the binding cleft, we measured the distance between several the C1 domain residues and the phorbol ester during the MD simulations. In the C1b domain-phorbol ester complex, H7 of phorbol-13-O-acetate formed a hydrogen bond with the carboxyl group of Lys[9] and O20 formed a hydrogen bond with the carboxyl group of Thr[12], which is a conserved residue among most C1 domains (Fig. 11). The distance between these phorbol ester atoms and the corresponding homologous residues in C1a WT, C1a P9K, and C1b K9P was plotted over 5.0 ns of the MD simulations (Fig. 11). For C1a WT, there were huge fluctuations during MD simulation and the distance increased significantly as the phorbol ester moved away from its first docked position. However, in C1a P9K, the corresponding distance was slightly reduced initially and then was maintained uniformly during the rest of the simulation period. This indicates that the phorbol ester docked C1a P9K is more stable than C1a WT. For C1b WT and C1b K9P, C1b WT showed reduced distances as compared to C1b K9P except during the 2.2 to 2.6 ns when more fluctuation of the Lys[9]-H7 distance was observed, indicating overall higher stability for the former.

In summary, our simulation results show that residues at position 9 of C1a and C1b contribute to these domains' affinity for phorbol ester. The relative contribution of the residues Pro[9] and Lys[9] toward the affinity will of course vary in the presence of lipids which was not considered in the simulation systems. The functional studies previously mentioned, of course, were conducted with the tertiary complex of C1 domain-ligand-lipid bilayer.

4. Discussion

The central role of protein kinases in cellular regulation and their prominent involvement in cancer and other disease processes has driven intense interest in the development of kinase targeted therapeutic agents. A critical challenge, however, is the high conservation of the ATP-binding site together with the size of the cellular kinome [23, 43]. In the case of protein kinase C family members, a complementary strategy has been to target its regulatory domain [44]. Here, the modest number of proteins with C1 domains along with the existence of multiple classes of natural products with high affinity for the C1 domains provide important advantages. Further opportunity is afforded by the complexity of the system, where specificity of interaction is provided not only by the ligand – C1 domain interactions but also by the membrane phospholipids which provide the third element of the binding complex. Reflecting these and other factors, the C1 domain targeted ingenol 3-angelate (Picato™, PEP005, ingenol mebutate) has been approved by the FDA for treatment of actinic keratosis, bryostatin 1 has been and is the subject of clinical trials for cancer and Alzheimer's disease, and prostratin has potential for overcoming the resistance to therapy of cells latently bearing HIV.

As part of this effort, understanding the differences in function of the individual C1 domains of PKC isoforms and of the C1 domains of the other families of proteins with DAG/phorbol ester responsive C1 is of great importance. One emerging concept is that the subdivision of C1 domains into "typical", i.e. DAG/phorbol ester binding, and "atypical", i.e. not binding DAG/phorbol ester, is simplistic. Rather, there is a continuum of affinities. At the one end, there are those C1 domains that bind with high affinity to DAG/phorbol ester and mediate physiological response to these ligands. The C1b domain of PKCθ, with an affinity of 1.6 nM for PDBu is an example. A second group of C1 domains still bind with measurable affinity, which is probably too low for regulation by physiological levels of DAG but may suffice for manipulation by pharmacological agents. As described here, the C1a domain of PKCθ, with an affinity for PDBu of 250 nM, is one example; the single C1 domain of RasGRP2 with an affinity of 2900 nM is one step weaker still [45]. The next group comprises those C1 domains without measurable binding affinity, like the C1 domains of PKCι/ζ and Vav1, which retain the appropriate geometry of the binding cleft but possess inappropriate charges along the rim of the binding cleft for proper membrane interaction [46, 47]. Finally, there are those C1 domains which no longer retain the binding cleft geometry, such as the C1 domain of Raf. Such differences represent an opportunity. We have described, for example, first generation derivatives of DAG-lactones that can begin to exploit the anomalous residues along the binding rim of the C1 domains of PKCι/ζ and of Vav1 [46, 47].

The C1a and C1b domains of PKCθ illustrate another important concept, that the influence of specific residues within the C1 domain structure cannot be assessed in isolation but only in the context of the other residues in the domain. While Pro in position 9 of the C1a domain caused a 70-fold loss of binding potency compared to a Lys in that position, in the C1b domain its effect was much more modest, with only a 7-fold decrease. Computer modeling fails to show a large influence of Pro[9] versus Lys[9] on the structure of the binding cleft,

arguing that it probably exerts its effect predominantly at the level of the ternary complex with the lipid bilayer.

PKCθ is most closely related to PKCδ, and we have discussed above the conflicting conclusions using different technical approaches about the relative contributions of the C1a and C1b domains of PKCδ to its response to DAG/phorbol ester. Our translocation results reported here found no positive contribution of the C1a domain to translocation in response to phorbol ester even in the construct with twin C1a domains. In contrast, the corresponding construct for PKCδ showed weak translocation in response to PMA and displayed a binding affinity of 12 nM, compared to 2.9 nM for the wild-type PKCδ [10]. While PKCθ is more closely related to PKCδ than to other PKC family members, this difference in the C1a domains remains an important distinction.

Although the initial concept of C1 domains was that they represented motifs for binding DAG/phorbol ester, the emerging view is that C1 domains represent interaction domains typically functioning both in the absence as well as in the presence of DAG/phorbol ester. Crystallographic structural determinations have shown that for PKCβII [48], for RasGRP1 [49], and for β2-chimaerin [50] the C1 domain binding cleft is interacting intramolecularly with other residues in the protein structure when in the unliganded state. Ligand would thus stabilize an alternative, intermolecular interaction of the C1 domain with membranes, with consequent loss of the stabilizing influence of the C1 domain on the folded structure of the inactive protein. Consistent with this understanding, disruption of the intramolecular interactions of the C1 domain with its interacting partners on the folded protein promote activation [48, 51]. From this perspective, the C1 domains with limited or absent DAG/phorbol ester binding activity presumably are mainly functioning as intramolecular binding motifs to stabilize the folded protein. The C1 domain of RasGRP2, which fails to bind phorbol ester, provides an intermediate example where it still can promote membrane stabilization of the active protein, albeit not in a phorbol ester dependent manner [52]. The atypical C1 domain of Vav1 provides an example of where its intramolecular interactions have been characterized [53] but where a regulatory function for the C1 domain with disruption of these interactions has not been described.

The C1a domain of PKCθ fits into the pattern. We found that deletion of the C1a domain of PKCθ sensitized the protein to translocation in response to phorbol ester. Likewise, Melowic et al. [17] described how mutations which were postulated to be disruptive of intramolecular interactions in either the C1a or C1b domains enhanced enzyme activity to a similar extent, despite their very different affinities for phorbol ester.

We have discussed above how the C1 regulatory domains may provide an attractive route for therapeutic targeting of PKC. One potential strategy for obtaining yet further selectivity is to exploit the differences in the tandem C1 domains of different PKC isoforms through bivalent ligands. These could exploit both the differences in spacing between the C1a and C1b domains of the classic PKCs, the novel PKCs and the PKDs and further distinguish between tandem C1 domains versus the single C1 domains of the other classes of signaling proteins with C1 domains. Further selectivity could be captured with bivalent ligands with one ligand binding moiety selective for a specific C1a domain and the other moiety selective for the

specific C1b domain, exploiting the differences between specific C1a and C1b domains such as those characterized here for PKCθ. Exciting early strides have been made exploring such approaches although significant challenges remain [54, 55].

Acknowledgments

References

[1]. Hurley JH, Newton AC, Parker PJ, Blumberg PM, Nishizuka Y, Taxonomy and function of C1 protein kinase C homology domains, Protein Sci 6 (2) (1997) 477–480, 10.1002/pro.5560060228. [PubMed: 9041654]

[2]. Nishizuka Y, The role of protein kinase C in cell surface signal transduction and tumor promotion, Nature 308 (5961) (1984) 693. [PubMed: 6232463]

[3]. Cho W, Stahelin RV, Membrane-protein interactions in cell signaling and membrane trafficking, Annu. Rev. Biophys. Biomol. Struct 34 (2005) 119–151, 10.1146/annurev.biophys. 33.110502.133337. [PubMed: 15869386]

[4]. Hansra G, Bornancin F, Whelan R, Hemmings BA, Parker PJ, 12-O-Tetradecanoylphorbol-13-acetate-induced dephosphorylation of protein kinase C alpha correlates with the presence of a membrane-associated protein phosphatase 2A heterotrimer, J. Biol. Chem 271 (51) (1996) 32785–32788. [PubMed: 8955114]

[5]. Young S, Parker PJ, Ullrich A, Stabel S, Down-regulation of protein kinase C is due to an increased rate of degradation, Biochem. J 244 (3) (1987) 775–779 [PubMed: 3446191]

[6]. Hubbard SR, Bishop WR, Kirschmeier P, George SJ, Cramer SP, Hendrickson WA, Identification and characterization of zinc binding sites in protein kinase C, Science 254 (5039) (1991) 1776–1779. [PubMed: 1763327]

[7]. Quest AF, Bloomenthal J, Bardes ES, Bell RM, The regulatory domain of protein kinase C coordinates four atoms of zinc, J. Biol. Chem 267 (14) (1992) 10193–10197. [PubMed: 1577787]

[8]. Giorgione JR, Lin JH, McCammon A, Newton AC, Increased membrane affinity of the C1 domain of protein kinase Cδ compensates for the lack of involvement of its C2 domain in membrane recruitment, J. Biol. Chem 281 (3) (2006) 1660–1669, 10.1074/jbc.M510251200. [PubMed: 16293612]

[9]. Dries DR, Gallegos LL, Newton AC, A single residue in the C1 domain sensitizes novel protein kinase C isoforms to cellular diacylglycerol production, J. Biol. Chem 282 (2) (2007) 826–830, 10.1074/jbc.C600268200. [PubMed: 17071619]

[10]. Pu Y, Garfield SH, Kedei N, Blumberg PM, Characterization of the differential roles of the twin C1a and C1b domains of protein kinase Cδ, J. Biol. Chem 284 (2) (2009) 1302–1312, 10.1074/jbc.M804796200. [PubMed: 19001377]

[11]. Szallasi Z, Bogi K, Gohari S, Biro T, Acs P, Blumberg PM, Non-equivalent roles for the first and second zinc fingers of protein kinase Cδ, J. Biol. Chem 271 (31) (1996) 18299–18301. [PubMed: 8702464]

[12]. Bogi K, Lorenzo PS, Szallasi Z, Acs P, Wagner GS, Blumberg PM, Differential selectivity of ligands for the C1a and C1b phorbol ester binding domains of protein kinase Cδ: possible correlation with tumor-promoting activity, Cancer Res 58 (7) (1998) 1423–1428. [PubMed: 9537243]

[13]. Zhang G, Kazanietz MG, Blumberg PM, Hurley JH, Crystal structure of the cys2 activator-binding domain of protein kinase C delta in complex with phorbol ester, Cell 81 (6) (1995) 917–924. [PubMed: 7781068]

[14]. Stewart MD, Cole TR, Igumenova TI, Interfacial partitioning of a loop hinge residue contributes to diacylglycerol affinity of conserved region 1 domains, J. Biol. Chem 289 (40) (2014) 27653–27664, 10.1074/jbc.M114.585570. [PubMed: 25124034]

[15]. Das J, Rahman GM, C1 domains: structure and ligand binding properties, Chem. Rev 114 (24) (2014) 12108–15131, 10.1021/cr300481j. [PubMed: 25375355]

[16]. Shindo M, Irie K, Nakahara A, Ohigashi H, Konishi H, Kikkawa U, Fukuda H, Wender PA, Toward the identification of selective modulators of protein kinase C (PKC) isozymes: establishment of a binding assay for PKC isozymes using synthetic C1 peptide receptors and identification of the critical residues involved in the phorbol ester binding, Bioorg. Med. Chem 9 (8) (2001) 2073–2081. [PubMed: 11504643]

[17]. Melowic HR, Stahelin RV, Blatner NR, Tian W, Hayashi K, Altman A, Cho W, Mechanism of diacylglycerol-induced membrane targeting and activation of protein kinase C theta, J. Biol. Chem 282 (29) (2007) 21467–21476, 10.1074/jbc.M700119200. [PubMed: 17548359]

[18]. Arendt CW, Albrecht B, Soos TJ, Littman DR, Protein kinase C-theta: signaling from the center of the T-cell synapse, Curr. Opin. Immunol 14 (3) (2002) 323–330. [PubMed: 11973130]

[19]. Isakov N, Altman A, Protein kinase C(theta) in T cell activation, Annu. Rev. Immunol 20 (2002) 761–794. [PubMed: 11861617]

[20]. Healy AM, Izmailova E, Fitzgerald M, Walker R, Hattersley M, Silva M, Siebert E, Terkelsen J, Picarella D, Pickard MD, LeClair B, Chandra S, Jaffee B, PKC-theta-deficient mice are protected from Th1-dependent antigen-induced arthritis, J. Immunol 177 (3) (2006) 1886–1893. [PubMed: 16849501]

[21]. Salek-Ardakani S, So T, Halteman BS, Altman A, Croft M, Differential regulation of Th2 and Th1 lung inflammatory responses by protein kinase C theta, J. Immunol 173 (10) (2004) 6440–6447. [PubMed: 15528385]

[22]. Salek-Ardakani S, So T, Halteman BS, Altman A, Croft M, Protein kinase C theta controls Th1 cells in experimental autoimmune encephalomyelitis, J. Immunol 175 (11) (2005) 7635–7641. [PubMed: 16301673]

[23]. Manning G, Whyte DB, Martinez R, Hunter T, Sudarsanam S, The protein kinase complement of the human genome, Science 298 (5600) (2002) 1912–1934, 10.1126/science.1075762. [PubMed: 12471243]

[24]. Cooke DW, Plotnick L, Type 1 diabetes mellitus in pediatrics, Pediatr. Rev 29 (11) (2008) 374–384 (quiz 385), 10.1542/pir.29-11-374. [PubMed: 18977856]

[25]. Marsland BJ, Soos TJ, Späth G, Littman DR, Kopf M, Protein kinase C theta is critical for the development of in vivo T helper (Th)2 cell but not Th1 cell responses, J. Exp. Med 200 (2) (2004) 181–189, 10.1084/jem.20032229. [PubMed: 15263025]

[26]. Giannoni F, Lyon AB, Wareing MD, Dias PB, Sarawar SR, Protein kinase C theta is not essential for T-cell-mediated clearance of murine gammaherpesvirus 68, J. Virol 79 (11) (2005) 6808–6813 (Erratum in: J Virol. 79(23):15004), 10.1128/JVI.79.11.6808-6813.2005. [PubMed: 15890920]

[27]. Blay P, Astudillo A, Buesa JM, Campo E, Abad M, García-García J, Miquel R, Marco V, Sierra M, Losa R, Lacave A, Braña A, Balbín M, Freije JM, Protein kinase C theta is highly expressed in gastrointestinal stromal tumors but not in other mesenchymal neoplasias, Clin. Cancer Res 10 (12 Pt 1) (2004) 4089–4095, 10.1158/1078-0432.CCR-04-0630. [PubMed: 15217944]

[28]. Duensing A, Joseph NE, Medeiros F, Smith F, Hornick JL, Heinrich MC, Corless CL, Demetri GD, Fletcher CD, Fletcher JA, Protein Kinase C theta (PKC theta) expression and constitutive activation in gastrointestinal stromal tumors (GISTs), Cancer Res 64 (15) (2004) 5127–5131, 10.1158/0008-5472.CAN-04-0559. [PubMed: 15289315]

[29]. Kang GH, Kim KM, Park CK, Kang DY, PKC-theta expression in Ewing sarcoma/primitive neuroectodermal tumour and malignant peripheral nerve sheath tumour, Histopathology 55 (3) (2009) 368–369, 10.1111/j.1365-2559.2009.03368.x. [PubMed: 19723158]

[30]. Rahman GM, Shanker S, Lewin NE, Kedei N, Hill CS, Prasad BV, Blumberg PM, Das J, Identification of the activator-binding residues in the second cysteine-rich regulatory domain of protein kinase Cθ (PKCθ), Biochem. J 451 (1) (2013) 33–44, 10.1042/BJ20121307. [PubMed: 23289588]

[31]. Lewin NE, Blumberg PM, [3H]Phorbol 12,13-dibutyrate binding assay for protein kinase C and related proteins, Methods Mol. Biol 233 (2003) 129–156, 10.1385/1-59259-397-6:129. [PubMed: 12840504]

[32]. Rahman GM, Das J, Modeling studies on the structural determinants for the DAG/phorbol ester binding to C1 domain, J. Biomol. Struct. Dyn 33 (1) (2015) 219–232, 10.1080/07391102.2014.895679. [PubMed: 24666138]

[33]. Hess B, Kutzner C, van der Spoel D, Lindahl E, GROMACS 4: algorithms for highly efficient, load-balanced, and scalable molecular simulation, J. Chem. Theory Comput 4 (3) (2008) 435–447, 10.1021/ct700301q. [PubMed: 26620784]

[34]. Hornak V, Abel R, Okur A, Strockbine B, Roitberg A, Simmerling C, Comparison of multiple Amber force fields and development of improved protein backbone parameters, Proteins 65 (3) (2006) 712–725, 10.1002/prot.21123. [PubMed: 16981200]

[35]. Sousa da Silva AW, Vranken WF, ACPYPE - AnteChamber PYthon Parser interfacE, BMC. Res. Notes 5 (2012) 367, 10.1186/1756-0500-5-367. [PubMed: 22824207]

[36]. Jorgensen WL, Chandrasekhar J, Madura JD, Impey RW, Klein ML, Comparison of simple potential functions for simulating liquid water, J. Chem. Phys 79 (2) (1983) 926–935, 10.1063/1.445869.

[37]. Berendsen HJC, van Postma JPM, van Gunsteren WF, DiNola ARHJ, Haak JR, Molecular dynamics with coupling to an external bath, J. Chem. Phys 81 (8) (1984) 3684–3690, 10.1063/1.448118.

[38]. Berk H, Bekker H, Berendsen HJC, Fraaije JGEM, LINCS: a linear constraint solver for molecular simulations, J. Comput. Chem 18 (12) (1997) 1463–1472, 10.1002/(SICI)1096-987X(199709)18:12<1463:AID-JCC4>3.0.CO;2-H.

[39]. Essmann U, Perera L, Berkowitz ML, Darden T, Lee H, Pedersen LG, A smooth particle mesh Ewald method, J. Chem. Phys 103 (19) (1995) 8577–8593, 10.1063/1.470117.

[40]. Kazanietz MG, Areces LB, Bahador A, Mischak H, Goodnight J, Mushinski JF, Blumberg PM, Characterization of ligand and substrate specificity for the calcium-dependent and calcium-independent protein kinase C isozymes, Mol. Pharmacol 44 (2) (1993) 298–307. [PubMed: 8355667]

[41]. Stahelin RV, DIgman MA, Medkova M, Ananthanarayanan B, Rafter JD, Melowic HR, Cho W, Mechanism of diacylglycerol-induced membrane targeting and activation of protein kinase Cδ, J. Biol. Chem 279 (28) (2004) 29501–29512, 10.1074/jbc.M403191200. [PubMed: 15105418]

[42]. Stewart MD, Morgan B, Massi F, Igumenova TI, Probing the determinants of diacylglycerol binding affinity in the C1B domain of protein kinase Cα, J. Mol. Biol 408 (5) (2011) 949–970, 10.1016/j.jmb.2011.03.020. [PubMed: 21419781]

[43]. Fleuren ED, Zhang L, Wu J, Daly RJ, The kinome "at large" in cancer, Nat. Rev. Cancer 16 (2) (2016) 83–98, 10.1038/nrc.2015.18. [PubMed: 26822576]

[44]. Blumberg PM, Kedei N, Lewin NE, Yang D, Czifra G, Pu Y, Peach ML, Marquez VE, Wealth of opportunity – the C1 domain as a target for drug development, Curr. Drug Targets 9 (8) (2008) 641–652 [PubMed: 18691011]

[45]. Czikora A, Lundberg DJ, Abramovitz A, Lewin NE, Kedei N, Peach ML, Zhou X, Merritt RC Jr., Craft EA, Braun DC, Blumberg PM, Structural basis for the failure of the C1 domain of Ras guanine nucleotide releasing protein 2 (RasGRP2) to bind phorbol ester with high affinity, J. Biol. Chem 291 (21) (2016) 11133–11147, 10.1074/jbc.M116.725333. [PubMed: 27022025]

[46]. Geczy T, Peach ML, El Kazzouli S, Sigano DM, Kang JH, Valle CJ, Selezneva J, Woo W, Kedei N, Lewin NE, Garfield SH, Lim L, Mannan P, Marquez VE, Blumberg PM, Molecular basis for failure of "atypical" C1 domain of Vav1 to bind diacylglycerol/phorbol ester, J. Biol. Chem 287 (16) (2012) 13137–13158, 10.1074/jbc.M111.320010. [PubMed: 22351766]

[47]. Pu Y, Peach ML, Garfield SH, Wincovitch S, Marquez VE, Blumberg PM, Effects on ligand interaction and membrane translocation of the positively charged arginine residues situated along the C1 domain binding cleft in the atypical protein kinase C isoforms, J. Biol. Chem 281 (44) (2006) 33773–33788, 10.1074/jbc.M606560200. [PubMed: 16950780]

[48]. Leonard TA, Rozcki B, Saidi LF, Hummer G, Hurley JH, Crystal structure and allosteric activation of protein kinase C βII, Cell 144 (1) (2011) 55–66, 10.1016/j.cell.2010.12.013. [PubMed: 21215369]

[49]. Iwig JS, Vercoulen Y, Das R, Barros T, Limnander A, Che Y, Pelton JG, Wemmer DE, Roose JP, Kuriyan J, Structural analysis of autoinhibition in the Ras-specific exchange factor RasGRP1, Elife 2 (2013) e00813, , 10.7554/eLife.00813. [PubMed: 23908768]

[50]. Canagarajah B, Leskow FC, Ho JY, Mischak H, Saidi LF, Kazanietz MG, Hurley J, Structural mechanism for lipid activation of the Ras-specific GAP, beta2-chimaerin, Cell 119 (3) (2004) 407–418, 10.1016/j.cell.2004.10.012. [PubMed: 15507211]

[51]. Sosa MS, Lewin NE, Choi SH, Blumberg PM, Kazanietz MG, Biochemical characterization of hyperactive beta2-chimaerin mutants revealed an enhanced exposure of C1 and RasGAP domains, Biochemistry 48 (34) (2009) 8171–8178, 10.1021/bi9010623. [PubMed: 19618918]

[52]. Johnson JE, Goulding RE, Ding Z, Partovi A, Anthony KV, Beaulieu N, Tazminin G, Cornell RB, Kay RJ, Differential membrane binding and diacylglycerol recognition by C1 domains of RasGRPs, Biochem. J 406 (2) (2007) 223–236, 10.1042/BJ20070294. [PubMed: 17523924]

[53]. Rapley J, Tybulewicz VL, Rittinger K, Crucial structural role for the PH and C1 domains of the Vav1 exchange factor, EMBO Rep 9 (7) (2008) 655–661, 10.1038/embor.2008.80. [PubMed: 18511940]

[54]. Giorgione J, Hysell M, Harvey DF, Newton AC, Contribution of the C1A and C1B domains to the membrane interaction of protein kinase C, Biochemistry 42 (38) (2003) 11194–11202, 10.1021/bi0350046. [PubMed: 14503869]

[55]. Sridhar J, Wei ZL, Nowak I, Lewin NE, Ayres JA, Pearce LV, Blumberg PM, Kozikowski AP, New bivalent PKC ligands linked by a carbon spacer: enhancement in binding affinity, J. Med. Chem 46 (19) (2003) 4196–4204, 10.1021/jm0302041. [PubMed: 12954072]

```
C1 motif           HxxxxxxxxxxxxCxxCxxxxxxxxxxxxxxCxxCxxxxHxxCxxxxxxxC
PKCδ C1b    231    HRFKVHNYMSPTFCDHCGSLLWGLVKQGLKCEDCGMNVHHKCREKVANLC    280    Q05655
PKCδ C1a    159    HEFIATEFGQPTFCSVCKDFVWGLNKQGYKCRQCNAAIHKKCIDKIIGRC    208    Q05655
PKCθ C1b    232    HRFKVYNYKSPTFCEHCGTLLWGLARQGLKCDACGMNVHHRCQTKVANLC    281    Q04759
PKCθ C1a    160    HEFTATFFPQPTFCSVCHEFVWGLNKQGYQCRQCNAAIHKKCIDKVIAKC    209    Q04759
```

■ C1a mutated amino acid residues
■ C1b mutated amino acid residues

Fig. 1.

Amino acid sequence alignment of the C1 domains of the PKC (human) delta and theta isoforms. Amino acid residues in the C1a and C1b domains of PKCθ that were evaluated for their contributions to the PDBu binding activity of PKCθ are color coded. Residues in the C1a domain that were substituted with the corresponding residue in the C1b domain are shown in red. Residues in the C1b domain that were substituted with the corresponding residue in the C1a domain are shown in blue. The C1 consensus sequence is highlighted in yellow.
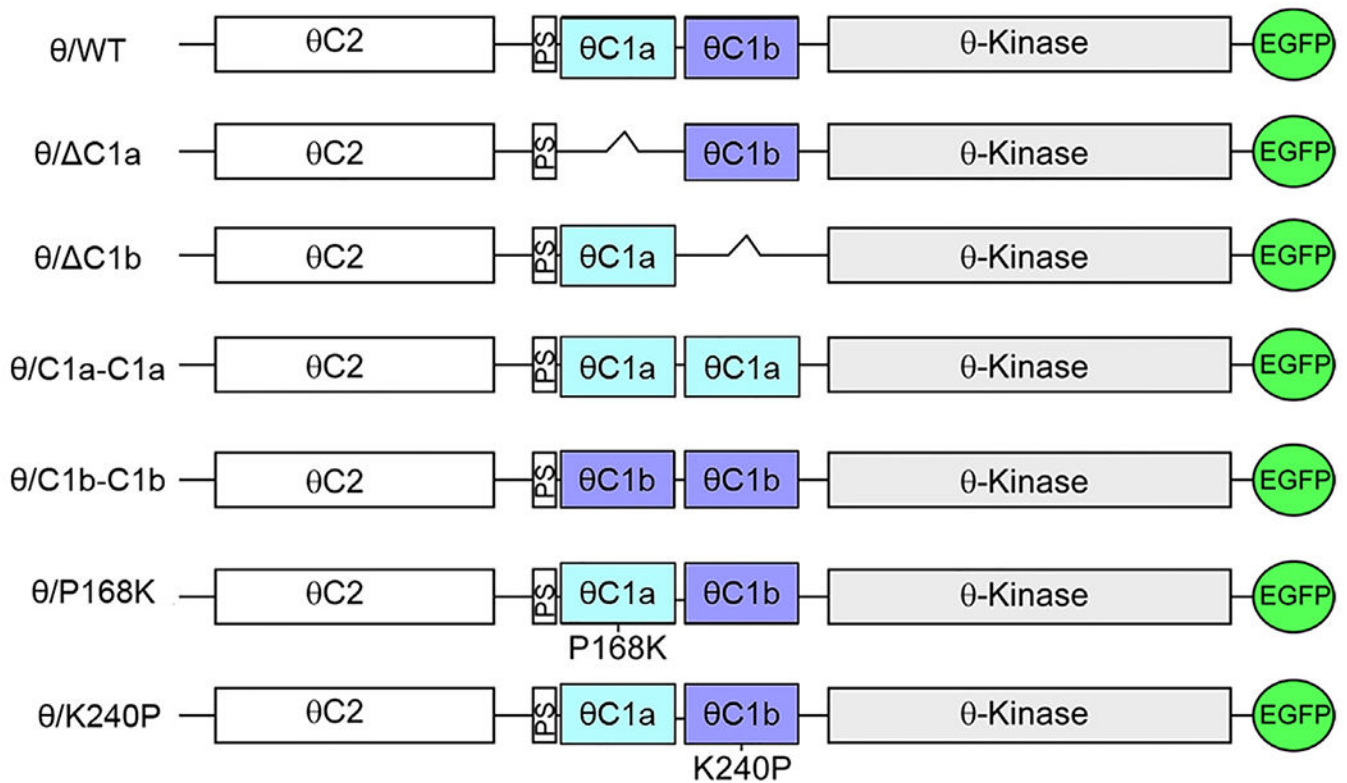
Fig. 2.
Schematic representation of the domain structure of θ/WT and sites of mutations and deletions. Mutants are referred as θ/ΔC1a in which θC1a was deleted, θ/ΔC1b in which θC1b was deleted, θ/C1a-C1a in which θC1b was substituted with θC1a, θ/C1b-C1b in which θC1a was substituted with θC1b, θ/P168K in which Pro168 of the θC1a domain was substituted with Lys and θ/K240P in which Lys240 of the θC1b domain was substituted with Pro.
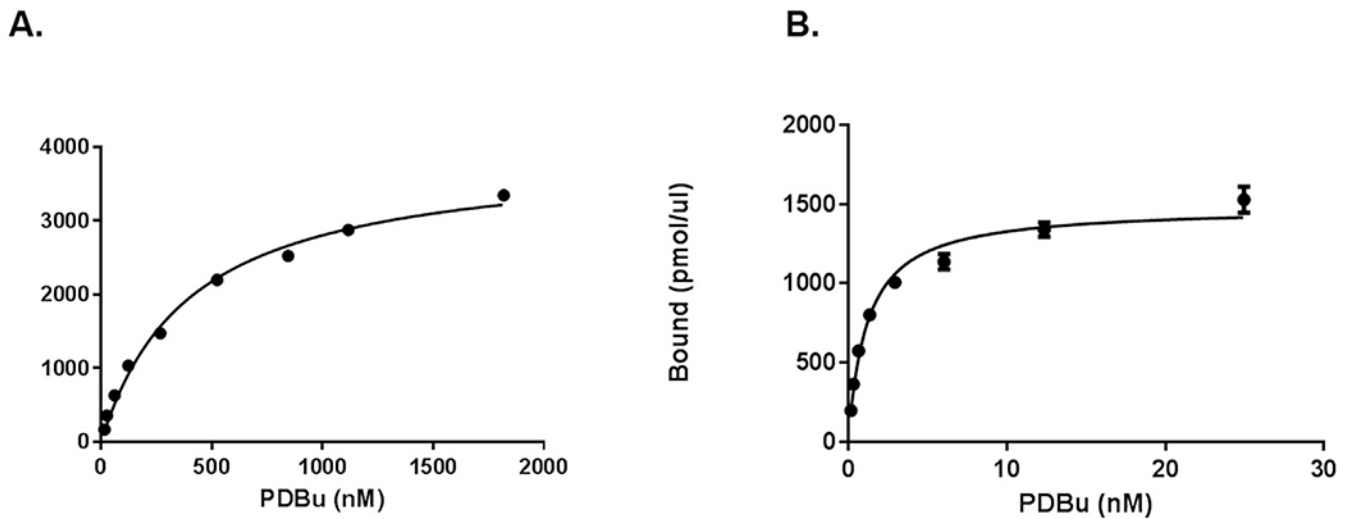
Fig. 3.
Binding of [³H]PDBu to the C1a and C1b domains of PKCθ. Binding of [³H]PDBu to the C1a (A) and the C1b (B) domains of PKCθ was measured in the presence of 100 μg/ml PS. Curves shown are from representative individual experiments. Points represent the mean value of the triplicate determinations at each PDBu concentration in the experiment. Error bars (±SEM) are shown when they exceed the size of the symbol. Three independent experiments were performed for each construct.
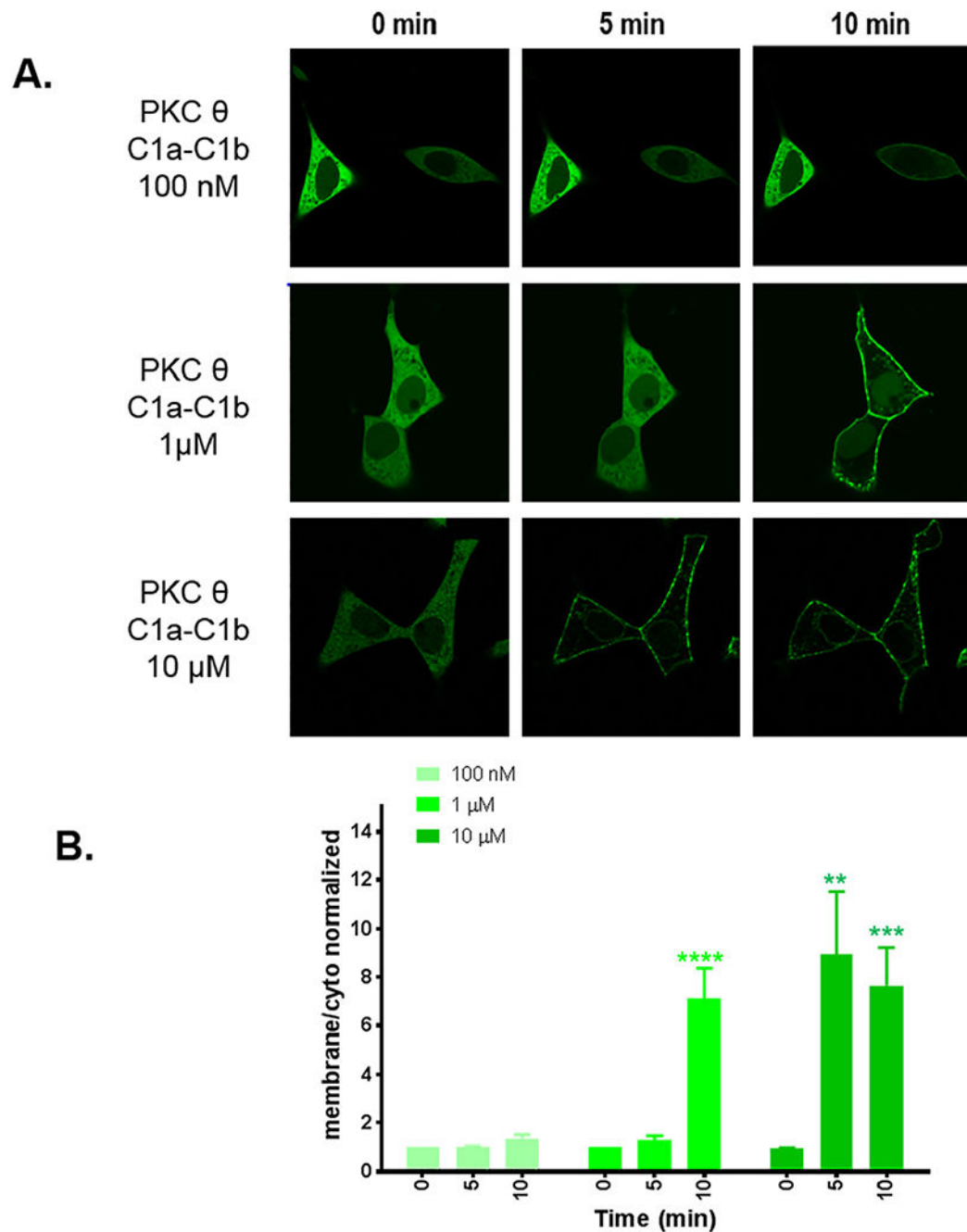
Fig. 4.

Translocation in response to PMA of the GFP-tagged wild type PKCθ in living LNCaP cells. Cells expressing GFP-tagged wild type PKCθ were treated with 100 nM, 1 µM and 10 µM PMA and the living cells were imaged by confocal microscopy as a function of time. A) Images shown are representative of three independent experiments. B) The ratios of the intensities for membrane/cytoplasm were calculated and normalized to the time 0 values. The increase in the membrane/cytoplasm ratio indicates translocation. Values represent the mean of the independent experiments. Bars±SEM. The increased translocation of wild type

PKCθ after 1 μM PMA treatment was significant with p < 0.0001; that after 10 μM PMA treatment was significant with p < 0.002 (5 min) and p < 0.0007 (10 min) (student's *t*-test).
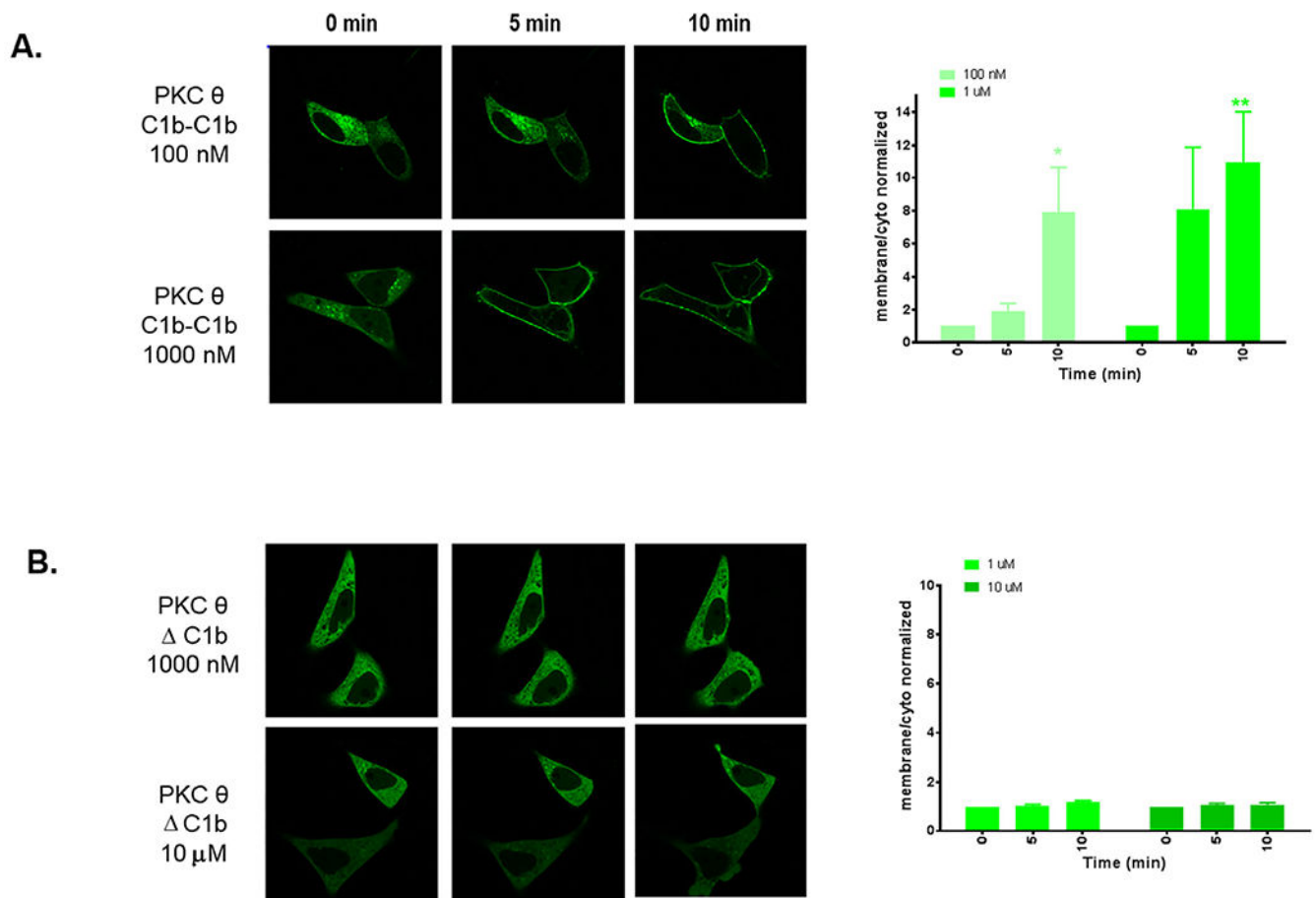
Fig. 5.
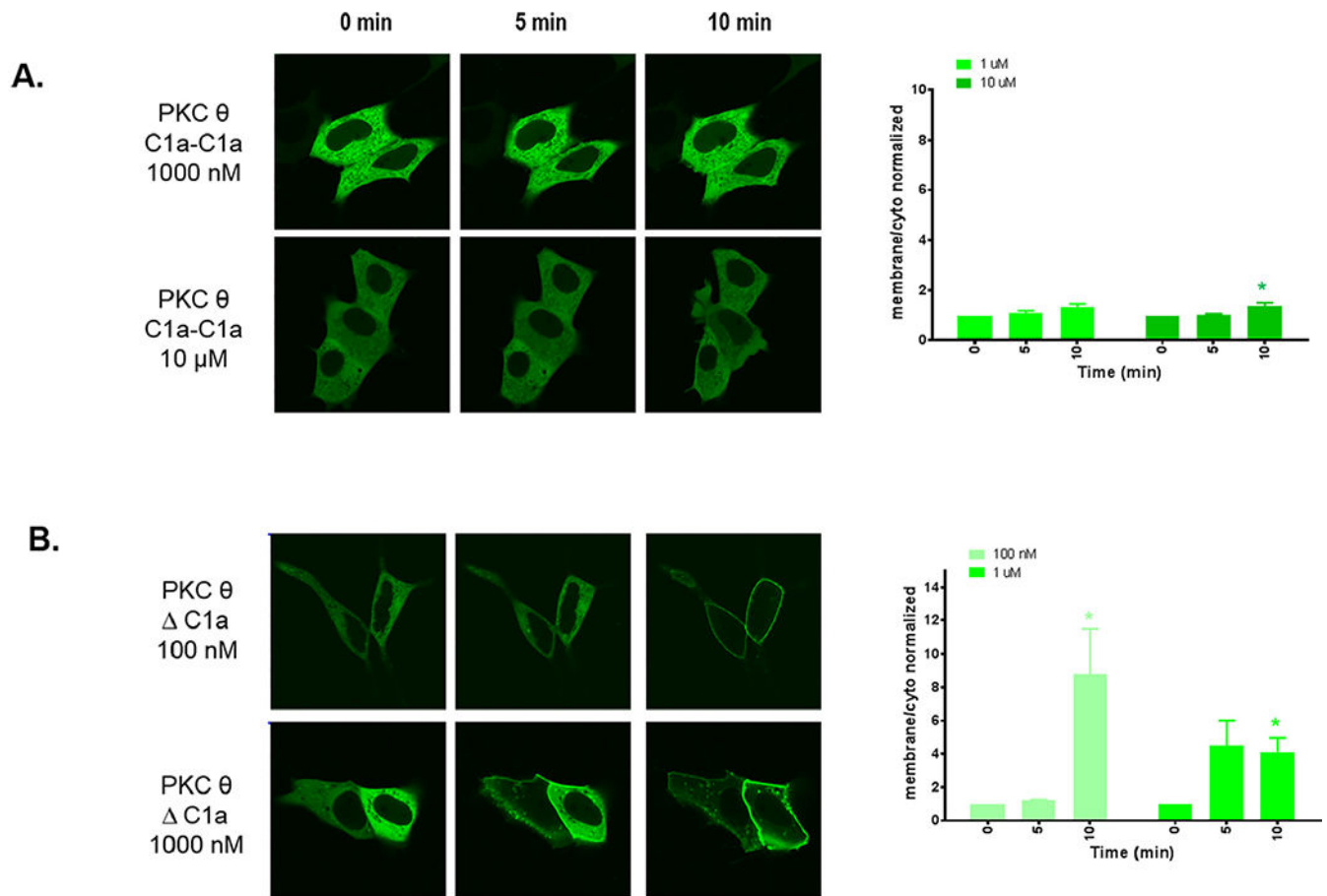Translocation in response to PMA of the GFP-tagged PKCθ C1b–C1b (A) chimera and
C1b (B) in living LNCaP cells. Cells expressing GFP-tagged C1b–C1b and C1b chimeras
of the full length PKCθ were treated with 100 nM, 1 μM and 10 μM PMA as indicated and
the living cells were imaged by confocal microscopy as a function of time. A-B) Images
shown are representative of three independent experiments and the ratios of the intensities
for membrane/cytoplasm were calculated and normalized to the time 0 values. The increase
in the membrane/cytoplasm ratio indicates translocation. Values represent the mean of the
independent experiments. Bars±SEM. The increased translocation of C1b–C1b chimera of
full length PKCθ after 100 nM PMA treatment was significant with p < 0.03; that after 1 μM
PMA treatment was significant with p < 0.003 (student's *t*-test).

Fig. 6.
Translocation in response to PMA of the GFP-tagged PKCθ C1a–C1a (A) chimera and
ΔC1a (B) in living LNCaP cells. Cells expressing the GFP-tagged C1a–C1a and ΔC1a
chimeras of the full length PKCθ were treated with 100 nM, 1 μM and 10 μM PMA. The
living cells were imaged by confocal microscopy as a function of time after PMA addition.
A-B) Images shown are representative of three independent experiments and the ratios of the
intensities for membrane/cytoplasm were calculated and normalized to the time 0 values.
The increase in the membrane/cytoplasm ratio indicates translocation. Values represent the
mean of the independent experiments. Bars±SEM. The increased translocation of ΔC1a
chimera of full length PKCθ after 100 nM PMA treatment was significant with $p < 0.01$;
that after 1 μM PMA treatment was significant with $p < 0.03$; and that of the C1a–C1a
chimera of full length PKCθ after 10 μM PMA treatment was significant with $p < 0.02$
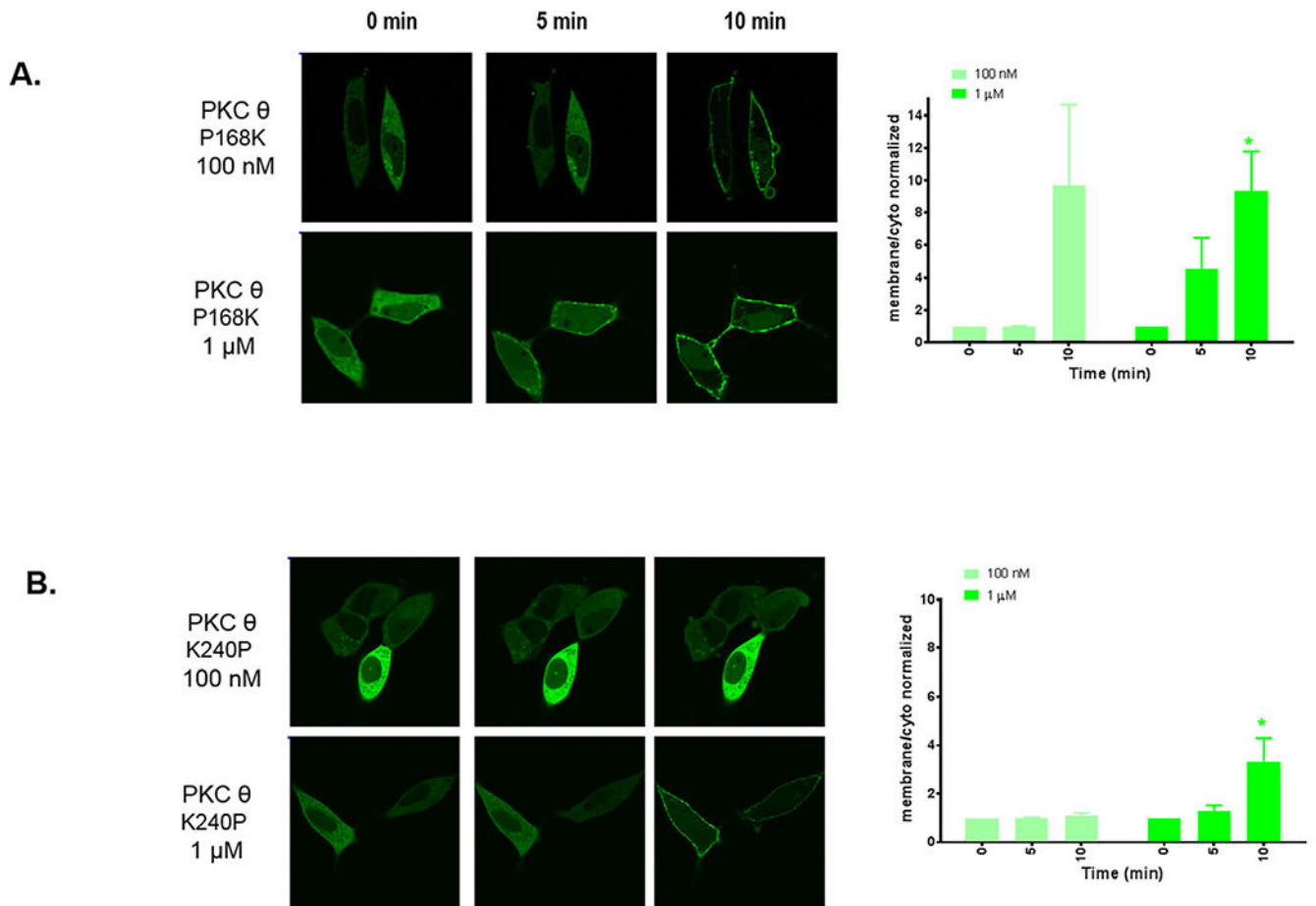(student's *t*-test).

Fig. 7.
Translocation in response to PMA of the GFP-tagged PKCθC1a/P168K (A) and C1b/K240P (B) mutants in living LNCaP cells. Cells expressing the GFP-tagged C1a and C1b mutants of full length PKCθ were treated with 100 nM and 1 μM PMA and the living cells were imaged by confocal microscopy as a function of time after PMA addition. A-B) Images shown are representative of three independent experiments and the ratios of the intensities for membrane/cytoplasm were calculated and normalized to the time 0 values. The increase in the membrane/cytoplasm ratio indicates translocation. Values represent the mean of the independent experiments. Bars±SEM. The increased translocation of C1a/P168K mutant was significant with $p < 0.02$; that of the C1b/K240P mutant at 1 μM PMA was significant with $p < 0.04$ (student's *t*-test).
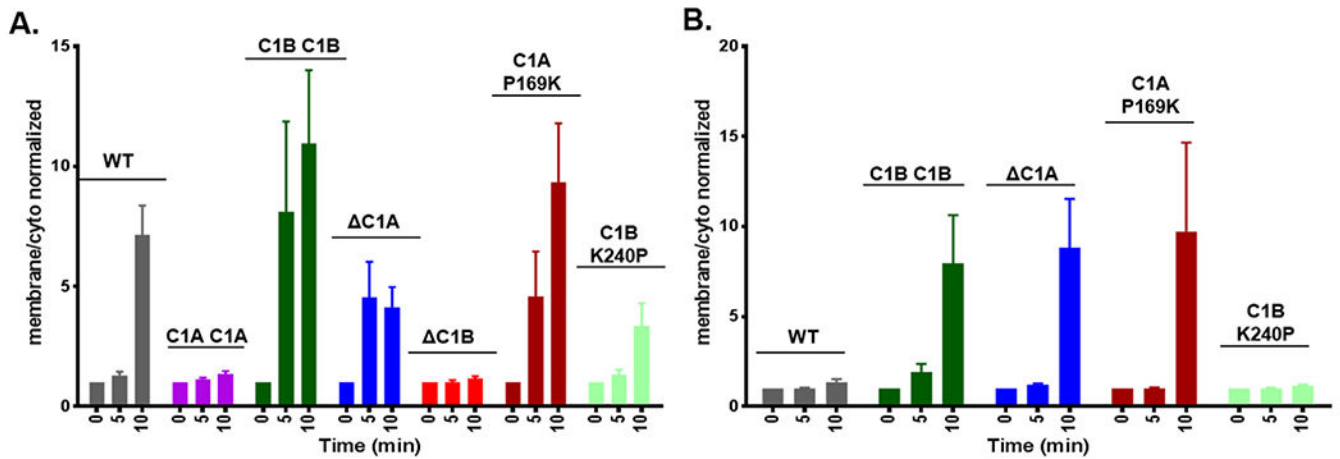
Fig. 8.

Summary of translocation in response to PMA of the GFP-tagged PKCθ constructs in living LNCaP cells. A) Time course of response upon treatment with 1 μM PMA for all constructs. B) Time course of response upon treatment with 100 nM PMA for those constructs that responded to 1 μM PMA. The ratios of the intensities for membrane/cytoplasm were calculated and normalized to the time 0 values. The increase in the membrane/cytoplasm ratio indicates translocation. Values represent the mean of the independent experiments. Bars ±SEM.
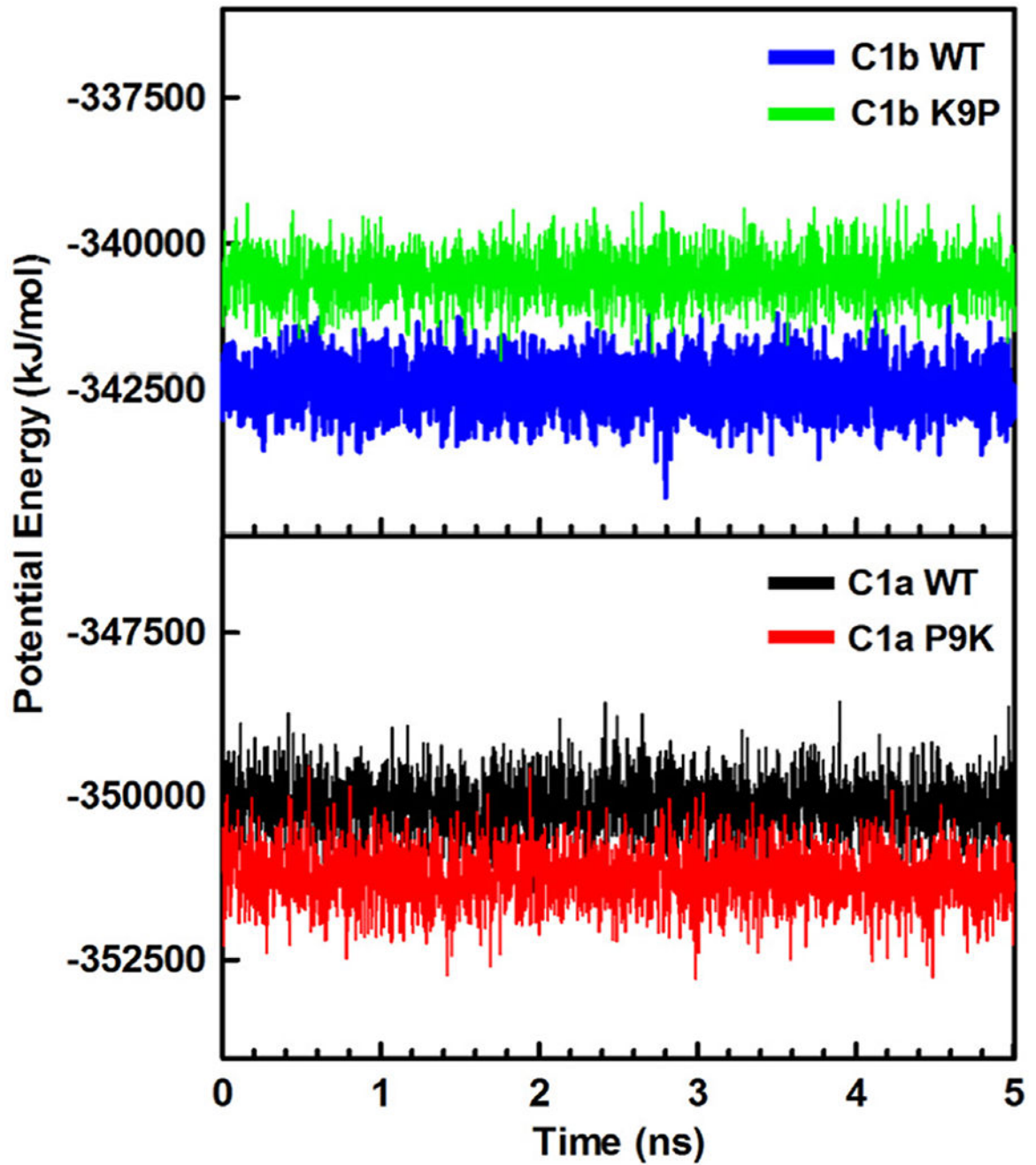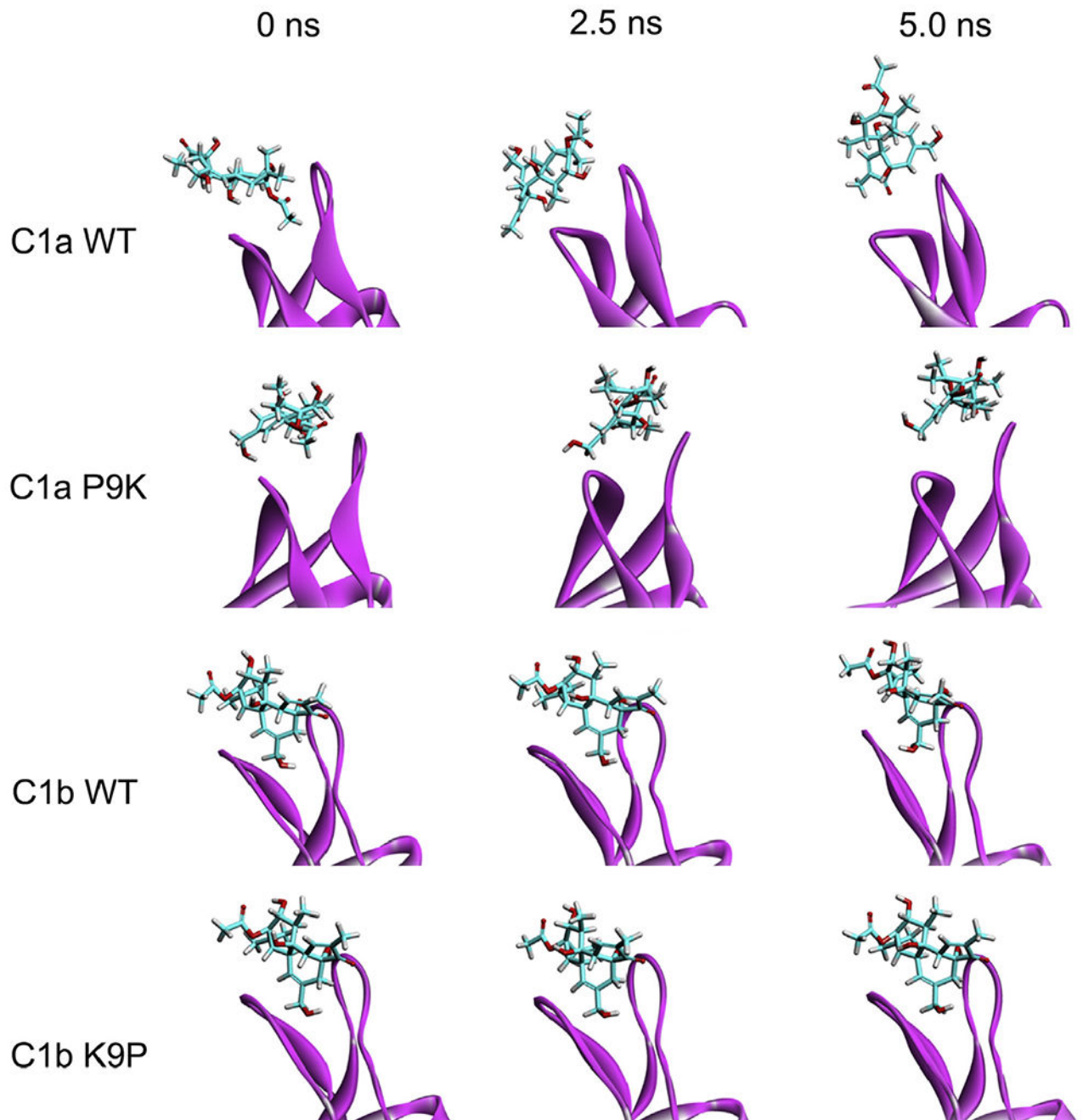
Fig. 9.
Plot of the potential energy of the C1 domain - phorbol 13-O-acetate complex during MD
simulation. Plots of potential energy that resulted from the MD simulations of the C1a WT,
C1a P9K, C1b WT, and C1b K9P during 5.0 ns.

Fig. 10.
Snapshots of the complexes of phorbol 13-O-acetate and the C1 domain at different time points of MD simulation. Snapshots were taken at 0 ns, 2.5 ns, and 5.0 ns. The C1 domain ribbon structure and the phorbol ester line structure are shown in magenta and cyan, respectively. The structures at 0 ns were taken after the systems were equilibrated before MD production.
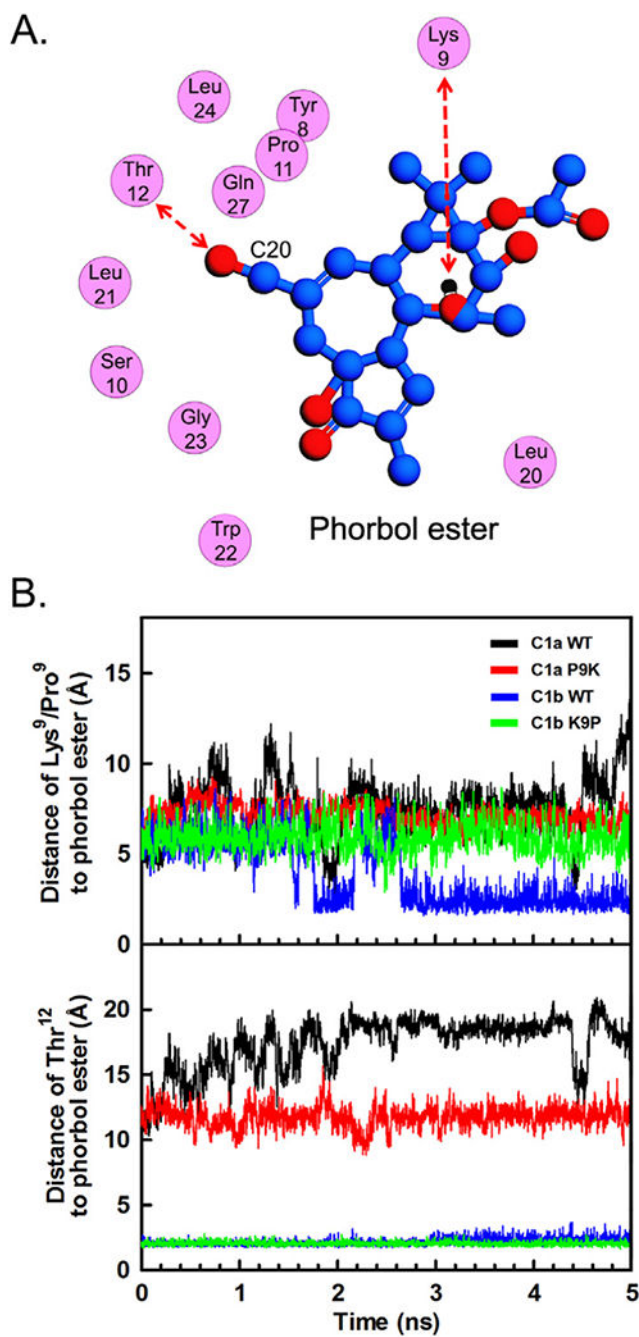
Fig. 11.
Interactions between phorbol 13-O-acetate and residues in the C1 domain. A. Distance between the phorbol ester and the residues of the C1b domain measured in Å for the MD simulation. The double headed arrows indicate the points of distance measurement. B. Plot showing the distance between Lys^9/Pro^9 and the phorbol ester, and between Thr^{12} and phorbol.

Table 1

Binding of [^{3}H]PDBu to the C1a and C1b domains of PKCθ. Individual wild type and mutant C1a and C1b domains were fused with GST, expressed in bacteria, and isolated. The binding affinities of the isolated proteins to [^{3}H]PDBu were measured in the presence of 100 μg/ml PS. Values represent the mean ± SEM (n = 3 independent experiments). NA, no measurable activity. Mutants with highest impact on binding are shown in bold.

Receptor	K_d [nM]
PKC theta C1a	
Wild type	254 ± 42
F8Y	NA
P9K	**3.60 ± 0.27**
Q10S	88 ± 9
S15E	116 ± 21
V16H	355 ± 36
H18G	1190 ± 350
E19T	514 ± 44
F20L	650 ± 200
V21L	81.9 ± 5.1
A36M	1840 ± 550
P9K/E19T	3.13 ± 0.43
P9K/V16H	1.73 ± 0.63
H18G/E19T	141 ± 20
N25A/K26R	NA
H18G/E19T/V21L	107 ± 17
PKC theta C1b	
Wild type	1.58 ± 0.54
K9P	**11.71 ± 0.28**
L21V	1.95 ± 0.33
M36A	2.00 ± 0.51
K9P/T19E	NA
K9P/M36A	35.90 ± 3.97